RESEARCH ARTICLE

NANO · MICRO small
www.small-journal.com

Photocatalytic CO_2 Reduction Using Homogeneous Carbon Dots with a Molecular Cobalt Catalyst

*Dongseok Kim, Subhajit Bhattacharjee, Erwin Lam, Carla Casadevall, Santiago Rodríguez-Jiménez, and Erwin Reisner**

A simple and precious-metal free photosystem for the reduction of aqueous CO_2 to syngas (CO and H_2) is reported consisting of carbon dots (CDs) as the sole light harvester together with a molecular cobalt bis(terpyridine) CO_2 reduction co-catalyst. This homogeneous photocatalytic system operates in the presence of a sacrificial electron donor (triethanolamine) in DMSO/H_2O solution at ambient temperature. The photocatalytic system exhibits an activity of 7.7 ± 0.2 $mmol_{syngas}$ g_{CDs}^{-1} (3.6 ± 0.2 $mmol_{CO}$ g_{CDs}^{-1} and 4.1 ± 0.1 $mmol_{H2}$ g_{CDs}^{-1}) after 24 hours of full solar spectrum irradiation (AM 1.5G). Spectroscopic and electrochemical characterization supports that this photocatalytic performance is attributed to a favorable association between CDs and the molecular cobalt catalyst, which results in improved interfacial photoelectron transfer and catalytic mechanism. This work provides a scalable and inexpensive platform for the development of CO_2 photoreduction systems using CDs.

1. Introduction

Photocatalytic valorization of the greenhouse gas CO_2 to CO is an appealing proposition to mitigate increasing anthropogenic CO_2 emissions.[1,2] The development of homogeneous and semi-heterogeneous colloidal systems that combine a photosensitizer with a fuel producing co-catalyst and operate in aqueous solution has garnered considerable attraction for the development of promising hybrid photocatalysts.[3–6] However, generally used photosensitizers promoting CO_2 reduction have several shortcomings such as expensive and chemically unstable Ru and Ir-based dyes,[7,8] toxic CdS,[9] organic dyes with low aqueous solubility and stability,[10] TiO_2 with limited visible light absorption,[11] and carbon nitride powders with hydrophobicity, low interfacial charge transfer and limited solubility,[12,13] restricting their potential for practical applications.

The creation of cost-effective, photostable, and highly active photocatalytic systems represents a major aim toward solar-to-fuel conversion.[14–16] Carbon dots (CDs) are carbon-based nanomaterials that hold significant promise due to their easy and scalable synthesis from inexpensive precursors, aqueous solubility, high extinction coefficient, and excellent photostability.[17,18] In this context, CDs have been studied as an alternative to conventional photosensitizers in combination with CO_2-to-CO reduction co-catalysts.[19,20] However, previous reports on light-driven CO_2 reduction using CDs required the incorporation of noble-metal catalysts[21] or heterogeneous photocatalysts, such as metal oxides,[22,23] metal- and covalent organic frameworks,[24,25] and carbon nitride,[26,27] resulting in higher cost, complexity, and low catalytic activity.

Homogeneous and precious-metal free photocatalytic CO_2 reduction using CDs has recently been introduced in our laboratory through modulating interfacial surface interactions.[28] However, our previous system required a fragile enzyme, formate dehydrogenase, as a co-catalyst for the CO_2-to-formate conversion, which limits more widespread utilization. Herein, we report a scalable, adaptable photocatalytic CO_2-to-syngas reduction system using CDs combined with a synthetic molecular cobalt co-catalyst, which demonstrates the use of CDs as the sole photosensitizer directly with a metal complex co-catalyst for the homogeneous photocatalytic reduction of CO_2 to syngas (**Figure 1a**).

2. Results and Discussion

Carboxylate-terminated N-doped carbon dots (g-N-CDs) were prepared as a light absorber according to a modified procedure (see Experimental Section).[29] g-N-CDs exhibit a broad, featureless UV–vis spectrum with a tailing into the visible range across the near-UV and the nitrogen-doped graphitic structure enhances the molar absorption coefficient as well as charge extraction ability of g-N-CDs, comparable to previous reports (Figure 1b; Table S1, Supporting Information).[29] In addition, the decoration of g-N-CDs with carboxylate groups offers a negative surface charge as confirmed by zeta potential measurements (Figure S1, Supporting Information). TEM imaging confirmed

D. Kim, S. Bhattacharjee, E. Lam, C. Casadevall, S. Rodríguez-Jiménez, E. Reisner
Yusuf Hamied Department of Chemistry
University of Cambridge
Lensfield Road, Cambridge CB2 1EW, UK
E-mail: reisner@ch.cam.ac.uk

The ORCID identification number(s) for the author(s) of this article can be found under https://doi.org/10.1002/smll.202400057

DOI: 10.1002/smll.202400057

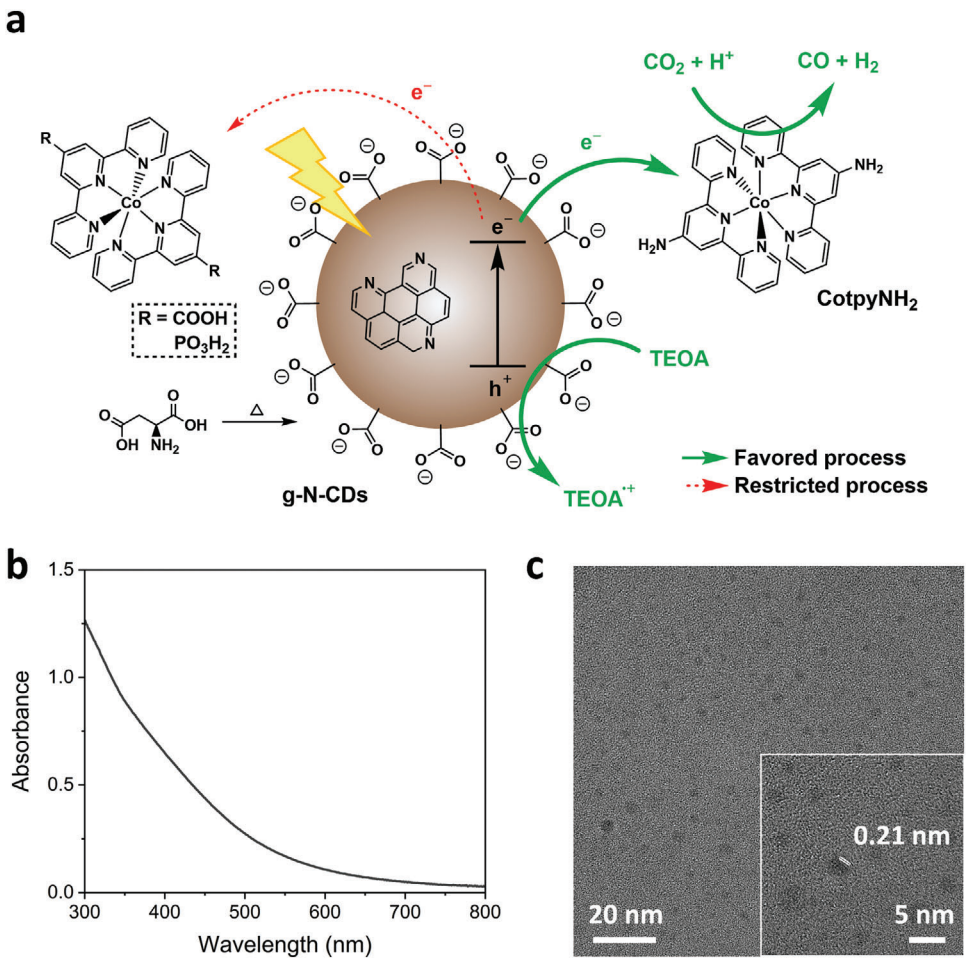

Figure 1. a) Schematic illustration of homogeneous photocatalytic CO_2 reduction system using carbon dots (g-N-CDs) and a molecular Co co-catalyst (CotpyR). b) UV–vis spectrum of g-N-CDs (0.05 mg mL^{-1}) in H_2O. c) TEM image of g-N-CDs with a high magnification (inset) for the graphitic spacing of the crystalline region.

the average diameter of g-N-CDs as 3.4 ± 0.6 nm with the (100) graphite plane of 0.21 nm (Figure 1c).[30]

A cobalt complex with two 4′-amine-2,2′:6′,2″-terpyridine ligands (denoted as $CotpyNH_2$) was synthesized in one step using a modified literature procedure from commercially available chemicals (see Experimental Section for full synthetic details and characterization and structure in Figure 1). The isolated, pre-assembled $CotpyNH_2$ was used for the experiments unless otherwise stated, but the metal complex can also be assembled in-situ from the cobalt tetrafluoroborate salt and the ligand (see below). The successful coordination between the terpyridine ligand and Co^{II} can be readily confirmed by metal-to-ligand charge transfer (MLCT) bands at ≈410, ≈460, and ≈510 nm using UV–vis spectroscopy (Figure S2, Supporting Information).[31] The NMR and mass spectra are consistent with the Co^{II} bis(terpyridine) complexes (Figures S3 and S4, Supporting Information).[32]

Photocatalytic performance of the CO_2 reducing g-N-CDs|$CotpyNH_2$ system was evaluated at 25 °C under simulated solar light irradiation (100 mW cm^{-2}, AM 1.5G). All experiments were carried out in a sealed borosilicate glass vial (V_{total} = 7.74 mL) charged with a DMSO:H_2O (1:1 v:v, 3 mL) solution containing a sacrificial electron donor (0.1 M unless otherwise stated). The vessel was purged with CO_2 containing 2% CH_4 as internal gas chromatography (GC) standard, and the produced gases were periodically monitored by analyzing the headspace by GC (see Experimental Section for details).

The photocatalytic system was optimized by varying several parameters, including type of sacrificial electron donors, solvents, solvent ratio, pH as well as photosensitizer and $CotpyNH_2$ loading (Figures S5–S10 and Tables S2–S6, Supporting Information). As a result of the systematic optimization, a maximal activity of 7.7 ± 0.2 $mmol_{syngas}$ g_{CDs}^{-1} (3.6 ± 0.2 $mmol_{CO}$ g_{CDs}^{-1} and 4.1 ± 0.1 $mmol_{H2}$ g_{CDs}^{-1}) was achieved after 24 h with g-N-CDs|$CotpyNH_2$ under full solar spectrum light irradiation at 25 °C with triethanolamine (TEOA) (0.1 M) in DMSO:H_2O (3 mL, 1:1 v:v) purged with CO_2. The highest $CotpyNH_2$ based turnover number for syngas (TON_{syngas}) was 15.9 ± 0.6 (TON_{CO} = 9.0 ± 0.4 and TON_{H2} = 6.9 ± 0.2) after 24 h. Among the screened solvents, aprotic DMSO, DMF, and DMA in combination with water showed higher photocatalytic activity than other organic:water mixtures. In addition, CDs synthesized via different methods (amorphous CDs

Table 1. Photocatalytic syngas (CO and H_2) production after 24 h of simulated solar light irradiation (100 mW cm^{-2}, AM 1.5G) at 25 °C with TEOA (0.1 M) in DMSO:H_2O (3 mL, 1:1 v:v) containing g-N-CDs (0.5 mg) and $CotpyNH_2$ (75 nmol) purged with CO_2, including exclusion control experiments. The photocatalytic activity and TON are blank (–) when the number of produced gases was less than the limit of detection (0.01 µmol).

Entry	Modification from standard conditions	$H_2 \pm \sigma$ [µmol]	Activity $\pm \sigma$ [$mmol_{H2}$ $(g_{CDs})^{-1}$]	TON (24 h) $\pm \sigma$ [mol_{H2} $(CotpyNH_2)^{-1}$]	Activity $\pm \sigma$ [μmol_{H2} $(g_{CDs})^{-1}$ h^{-1}] (after 6 h)	CO $\pm \sigma$ [µmol]	Activity $\pm \sigma$ [$mmol_{CO}$ $(g_{CDs})^{-1}$]	TON (24 h) $\pm \sigma$ [mol_{CO} $(CotpyNH_2)^{-1}$]	Activity $\pm \sigma$ [μmol_{CO} $(g_{CDs})^{-1}$ h^{-1}] (after 6 h)
1	None	0.39 ± 0.03	0.78 ± 0.56	5.18 ± 0.37	59.37 ± 6.84	0.65 ± 0.03	1.30 ± 0.58	8.66 ± 0.39	68.97 ± 7.95
2	No CDs	0.01 ± 0.01	0.022 ± 0.0067	0.15 ± 0.04	2.42 ± 0.073	< 0.01	–	–	–
3	No Co-catalysts	< 0.01	–	–	–	< 0.01	–	–	–
4	No electron donors	< 0.01	–	–	–	< 0.01	–	–	–
5	No light	< 0.01	–	–	–	< 0.01	–	–	–
6	No CO_2	0.35 ± 0.02	0.70 ± 0.04	4.65 ± 0.23	55.56 ± 3.73	< 0.01	–	–	–

(a-CDs), graphitic CDs (g-CDs), and cellulose derived CDs (α-cel CDs); see Experimental Section for details)[33] and other CO_2 reduction molecular co-catalysts (rhenium bipyridine and cobalt phthalocyanine)[34,35] were also employed, but their activity was significantly lower than that of g-N-CDs|$CotpyNH_2$ (Figures S11 and S12 and Tables S7 and S8, Supporting Information). Control exclusion experiments in the absence of co-catalyst, CD light absorber, CO_2, electron donor, and light, were systematically performed, showing no or negligible photocatalytic activity for CO_2 reduction (**Table 1**; Figures S13 and S14, Supporting Information).

We also found that a mixture of g-N-CDs, ligand ($tpyNH_2$), and cobalt tetrafluoroborate could perform the photocatalytic CO_2-to-syngas conversion efficiently without the need for pre-synthesis of the molecular catalyst. Thus, in-situ formation of $CotpyNH_2$ for photocatalysis is possible from commercially available chemicals, which facilitates scaling and more practical use in the future (Figure S15, Supporting Information). Isotopic labelling studies using $^{13}CO_2$ with gas phase product analysis by transmission IR spectroscopy were carried out after 24 h photocatalysis in DMSO:H_2O, confirming that the produced CO originated solely from CO_2 (Figure S16, Supporting Information).

After establishing the homogeneous photocatalytic hybrid system for CO_2 reduction, the long-term stability was investigated in DMSO:H_2O (3 mL, 1:1 v:v) containing g-N-CDs (0.5 mg) and $CotpyNH_2$ (75 nmol) with TEOA (0.1 M). The amount of produced syngas (H_2 and CO) continuously increased up to 60 h (**Figure 2a**). After 24 h, the photocatalytic rate (µmol g^{-1} h^{-1}) started to decay due to the limited stability of the molecular catalyst, and after ~50 h, the syngas production was nearly negligible. Nonetheless, the selectivity for CO was 65% throughout the long-term experiment, indicating that the molecular catalyst produced CO and H_2 with comparable selectivity regardless of the ongoing decomposition process. To confirm that the co-catalyst limits the lifetime of the system, fresh $CotpyNH_2$ (75 nmol) was added, and the solution re-purged with CO_2 after every 24 h of photocatalysis (Figure 2b). This allowed recovery and prolonged activity, and after five 24 h-cycles, the photocatalytic system maintained 90% and 73% of their activity for proton and CO_2 reduction, respectively. The activity was not recovered when the photosystem was only re-purged with CO_2 gas without adding fresh $CotpyNH_2$ (Figure S17, Supporting Information). These results confirm the photostability of g-N-CDs in the studied system for over 120 h.

To investigate the mode of decomposition of the co-catalyst, we have performed in-situ UV–vis spectroscopy studies to monitor the degradation during the photocatalytic CO_2 reduction reaction (Figure S18, Supporting Information). We found that

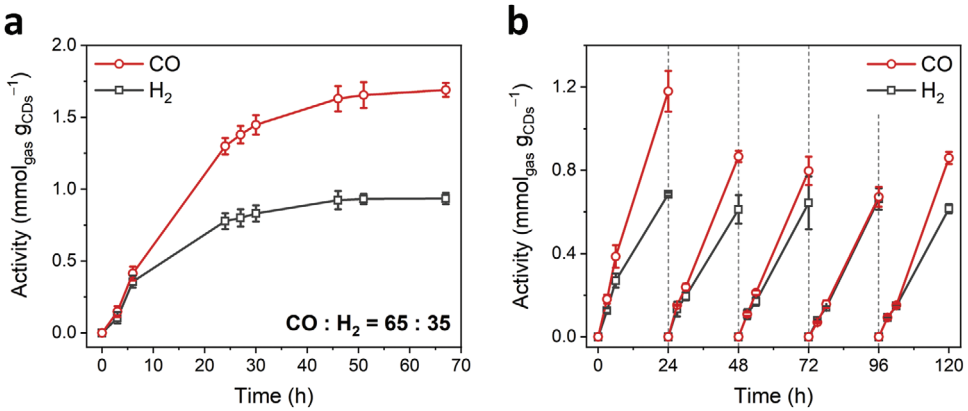

Figure 2. a) Photocatalytic syngas (CO and H_2) production for 67 h. b) Photocatalytic performance when $CotpyNH_2$ (75 nmol) and CO_2 was supplemented every 24 h. The reactions were conducted under simulated solar light irradiation (100 mW cm^{-2}, AM 1.5G) at 25 °C in CO_2-purged DMSO:H_2O (3 mL, 1:1 v:v) with TEOA (0.1 M) containing g-N-CDs (0.5 mg) and $CotpyNH_2$ (75 nmol).

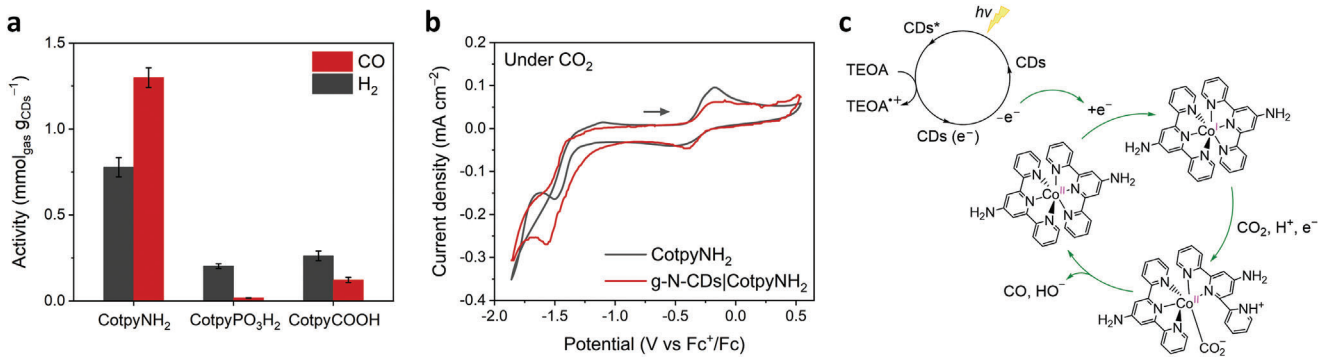

Figure 3. a) Photocatalytic syngas (CO and H_2) production after 24 h of simulated solar light irradiation (100 mW cm^{-2}, AM 1.5G) at 25 °C with TEOA (0.1 M) containing g-N-CDs (0.5 mg) and CotpyR (75 nmol) purged with CO_2. b) Cyclic voltammogram of 1 mg mL^{-1} of g-N-CDs and 1 mM of CotpyNH$_2$ in 0.1 M TBABF$_4$ under CO_2 atmospheres at 100 mV s^{-1}. All experiments were implemented in DMSO:H_2O (1:1 v:v) solution. c) Postulated mechanism for photocatalytic CO_2 reduction by the g-N-CDs|CotpyNH$_2$ system – the catalytic cycle is based on a literature report.[31]

the absorption at 345 nm, which is assigned to the red-shifted π–π^* transition of the aromatic tpy ligand by electron delocalization through the complexation to the Co ion,[36] was steadily decreased during 405 nm LED irradiation, presumably due to displacement of tpyNH$_2$ from the Co center. Moreover, the addition of $FeCl_3$ to the irradiated g-N-CDs|CotpyNH$_2$ system led to a gradual absorbance increase in the 500–600 nm range, which is associated with the formation of [$FeCl_3$tpy] complex under light irradiation (Figures S19 and S20, Supporting Information).[37] No absorption from the Fe complex was observed in the photocatalytically inactive systems, CotpyCOOH and CotpyPO$_3$H$_2$ (see Figure 1a; Figures S21 and S22, Supporting Information and below for more details). The terpyridine ligand loss was irreversible and remained even after turning off the LED for 60 min. In the absence of g-N-CDs, CotpyNH$_2$, or light, no significant changes were observed (Figures S23 and S24, Supporting Information). Thus, ligand displacement from the metal center reduces the activity of the Co catalyst and is likely to cause inactivation for the g-N-CDs|CotpyNH$_2$ system. This observation is consistent with previous reports that demonstrated a higher overpotential for CO_2 reduction required for the mono(terpyridine)-Co complex (not accessible for the photoexcited CDs) compared to the corresponding bis(terpyridine)-Co catalyst.[31,38]

Good photocatalytic activity of multi-component systems has previously been associated with favorable interfacial interactions between the photosensitizer and co-catalyst such as π–π conjugation,[39] H-bonding,[40] and electrostatic interactions.[28,41] To gain further insights into the CD-molecule interface, three cobalt(II) bis(terpyridine) complexes with different functional groups at the central 4'-terpyridine ring (R = NH$_2$, COOH, and PO$_3$H$_2$) (see Experimental Section for synthetic details) were studied (denoted as CotpyR with R = NH$_2$, COOH, and PO$_3$H$_2$) to govern the electrostatic interactions with the negatively charged g-N-CDs (Figure 1a). The highest photocatalytic activity for CO_2 reduction was exhibited with CotpyNH$_2$, which would be consistent with coulombic attraction between the two components (**Figure 3a**; Figure S25 and Table S9, Supporting Information). The strong association between g-N-CDs and CotpyNH$_2$ was further substantiated through the rapid formation of an aggregate in a mixture of g-N-CDs and CotpyNH$_2$ in DMSO:H_2O (1:1 v:v) solution (Figure S26a, Supporting Information), which was also confirmed by Fourier transform infrared (FT-IR) spectroscopy following filtration (Figure S26b, Supporting Information).

Photoluminescence quenching experiments showed that the emission intensity of g-N-CDs at λ_{ex} = 360 nm was gradually decreased as the amount of added CotpyR increased, indicating effective photoelectron transfer facilitating the photocatalytic reaction (Figure S27, Supporting Information). In addition, the Stern–Volmer constant (K_{SV}) showed a better association of CotpyNH$_2$ with g-N-CDs in a DMSO:H_2O (1:1 v:v) solution purged with CO_2, compared to the other CotpyR complexes, which is in agreement with a previous report showing the oxidative quenching of electrostatically bound CDs.[42] This result supports that faster electron transfer kinetics induced by the electrostatic interaction between g-N-CDs and CotpyNH$_2$ resulted in the higher photocatalytic performance of the g-N-CDs|CotpyNH$_2$ system.

Cyclic voltammetry studies were conducted to further explore the origin of the photocatalytic activity of the g-N-CDs|CotpyNH$_2$ system. First, the cyclic voltammograms of each CotpyR (1 mM) under N_2 in a DMSO:H_2O (1:1 v:v) solution containing 0.1 M tetrabutylammonium tetrafluoroborate (TBABF$_4$) as supporting electrolyte referenced against the ferrocene couple (Fc$^+$/Fc) showed two reversible electrochemical features (Figures S28 and S29, Supporting Information). Each feature was assigned to two metal-based processes, i) Co^{III}/Co^{II} and ii) Co^{II}/Co^{I} reduction consistent with previous reports.[38,43] CotpyR displays a further (third) electrochemical wave that is assigned to a ligand-based reduction (tpy/tpy$^{\bullet-}$ couple) and generates a Co^{I}(tpy$^{\bullet-}$) species associated with the catalytic cycle for CO_2 reduction (Figure S30, Supporting Information; orange arrows). The corresponding anodic wave (at potentials > −1.5 V vs Fc$^+$/Fc) was not observed, possibly due to the reduction of protons available abundantly in the semi-aqueous medium (see Table 1). Under a CO_2 atmosphere, a clear enhancement in the cathodic current density of the third wave was observed, which is attributed to the catalytic CO_2 reduction process, in agreement with previous reports.[38] No notable difference was observed in the two metal-based electrochemical features.

The electrochemical features of the assembled hybrid systems (g-N-CDs|CotpyR) were also investigated in a dark DMSO:H_2O (1:1 v:v) solution with 0.1 M $TBABF_4$ containing g-N-CDs (1 mg mL^{-1}) and CotpyR (1 mM) (Figure 3b; Figures S31 and S32, Supporting Information). A notable current enhancement and positively shifted onset potential of the Co^{II}/Co^{I} reduction wave at −1.5 V versus Fc^+/Fc was observed in the cyclic voltammogram for g-N-CDs|CotpyNH_2. The other two systems (g-N-CDs|CotpyCOOH and g-N-CDs|CotpyPO_3H_2) did not show these significant changes at the second reduction wave and catalysis was only initiated at the third reduction wave at lower potentials. The presence of an altered and improved catalytic activity is explained by a strong association of g-N-CDs and CotpyNH_2 via enhanced electrostatic interaction as compared to the other two systems, which is consistent with the Stern–Volmer analysis. Additionally, electrolysis at −1.5 V versus Fc^+/Fc was conducted using g-N-CDs|CotpyNH_2 to confirm that the reduction of Co^{II} to Co^{I} was engaged in CO_2 reduction (Figure S33, Supporting Information). Syngas (CO and H_2) was detected after 1 h of chronoamperometry, exhibiting 21% of FE for CO (the remaining FY was due to H_2 evolution). In the absence of g-N-CDs, the CO production was negligible for CotpyNH_2 with only 1% of FE. Moreover, no H_2 and CO was identified at a more positive potential (−0.6 V vs Fc^+/Fc) with g-N-CDs|CotpyNH_2.

From the results of the photoluminescence quenching, electrochemical analysis, and in-situ UV–vis absorption, we postulate that the favorable association of g-N-CDs and CotpyNH_2 improves the photoelectron transfer as well as catalytic mechanism and, thus, photocatalytic CO_2 reduction. The enhanced activity of CotpyNH_2 is presumably made possible by the association with g-N-CDs, which enables entering the catalytic cycle already upon the reduction of Co^{II} to Co^{I}, rather than the ligand-centered reduction (Figure 3c). This is in agreement with our previous report,[31] where a reduced $Co^{I}(tpy)_2$ species immobilized on a porous metal oxide electrode was directly involved in the CO_2 reduction mechanism via a proposed oxidative addition of CO_2 on the Co^{I} site and, subsequently, CO release. We therefore suggest that the favorable interaction between g-N-CDs and CotpyNH_2 can also promote such an altered alternative catalytic cycle (see Figure S30, Supporting Information) and thus requires a lower reductive potential for efficient photocatalytic CO_2 reduction with CotpyNH_2.

3. Conclusion

We have established a homogeneous photocatalytic CO_2-to-syngas reduction system using CDs as a sole light absorber in combination with a molecular 3d transition metal co-catalyst for CO_2 reduction. Photo-excited electron transfer between the g-N-CDs and CotpyNH_2 facilitated efficient CO_2 reduction with a maximal activity of 7.7 ± 0.2 $mmol_{syngas}\ g_{CDs}^{-1}$ (3.6 ± 0.2 $mmol_{CO}\ g_{CDs}^{-1}$ and 4.1 ± 0.1 $mmol_{H2}\ g_{CDs}^{-1}$) under simulated solar light irradiation after 24 h and systematic optimization. Physical characterization involving electrochemistry and spectroscopy supports that the favorable association assigned to an electrostatic interaction between g-N-CDs and CotpyNH_2 allows this specific photosensitizer-molecular catalyst hybrid system to attain significant photocatalytic activity for CO_2 reduction through two beneficial effects: i) association, presumably through electrostatic interactions, enhances photo-induced electron transfer at the g-N-CDs|CotpyNH_2 interface; ii) the favorable interaction changes the catalytic mechanism and enables the co-catalyst to enter the catalytic cycle already upon reduction of Co^{II} to Co^{I}, which occurs at an accessible potential for the photoexcited CD. Furthermore, as CDs can be prepared by a simple one-step pyrolysis procedure and the Co complex can also be simply self-assembled from commercially available chemicals, we also demonstrate a scalable and adaptable photocatalyst system that can in principle be prepared without a sophisticated chemical laboratory infrastructure. The simplicity of this multi-component system also invites using this system for high-throughput screening of CDs with different metal-ligand catalyst combinations to improve efficiency for photocatalytic CO_2 reduction and further mechanistic studies using in-situ spectroscopy in future studies.[44,45]

4. Experimental Section

Materials: All chemicals were obtained from commercial suppliers and used as received unless otherwise noted.

Synthesis of g-N-CDs: g-N-CDs were prepared according to a previous report.[29] Briefly, Aspartic acid (20 g) was put into a beaker and calcined at 320 °C (10 °C min^{-1}) for 100 h in air. Next, the sample was dissolved in water (400 mL) and NaOH (5 M) was added to neutralize the sample. After stirring for an hour, the pH of the solution was re-adjusted to 7 and kept stirring overnight. The obtained dark brown solution was filtered through a microfilter (0.22 µm) and isolated as a dark-brown powder upon freeze-drying.

Synthesis of Amorphous CDs (a-CDs), Graphitic CDs (g-CDs), and α-Cellulose Derived CDs (α-cel CDs): All three different types of CDs were synthesized as previously reported.[33] For a-CDs, citric acid (20 g) was put into a 250 mL beaker and kept for heating at specific conditions (40 h, 180 °C, 10 °C min^{-1}, air). A dark brown high-viscous product was obtained. Then, the samples were neutralized with 5 M NaOH and freeze-dried to isolate a-CDs. g-CDs were prepared through a two-step thermal treatment of citric acid. Citric acid (5 g) was thermally treated in air at 180 °C for 40 h and then pyrolyzed at 320 °C in air for 100 h. The graphitized product was dissolved in water and neutralized with NaOH (5 M). The reaction mixture was filtered by a 0.22 µm microfilter and then freeze-dried to obtain dark brown g-CDs. Lastly, α-cel CDs were synthesized upon thermal calcination of α-cellulose (10 g) at 320 °C in air for 100 h. The product was cooled to room temperature and used without further treatment.

Synthesis of CotpyR: CotpyR was synthesized according to reported procedures with some modifications.[31] A terpyridine ligand with a different functional group (2,2′:6′,2″-terpyridine-4′-phosphonic acid (tpyPO_3H_2), 2,2′:6′,2″-terpyridine-4′-carboxylic acid (tpyCOOH), and 2,2′:6′,2″-terpyridine-4′-amine (tpyNH_2) (9.60×10^{-5} mol), purchased from HetCat and $Co(BF_4)_2{\cdot}6H_2O$ (4.20×10^{-5} mol) were added in a Schlenk flask under a N_2 atmosphere and solubilized in MeOH (6 mL) purged with N_2. The solution was stirred for 24 h at room temperature. During the reaction, the color of the reaction mixture gradually turned to red-brown, attesting to the formation of the cobalt bis(terpyridine) complex. Next, ethanol (4 mL) was added, followed by diethyl ether to precipitate the complex. The solvent was decanted and the solid washed with diethyl ether. The product was collected by filtration under vacuum to isolate CotpyR complex as a dark red powder. Characterization of CotpyNH_2 is as follows: ^{1}H-NMR (500 MHz, CD_3CN): δH (ppm) = 107.93 (bs, H^a), 88.22 (s, H^b), 74.35 (s, H^c), 31.32 (s, H^d), 17.94 (s, H^e). EA (CHN combustion for C, H, and N and ICP-OES for B and Co): Calcd. for $C_{30}H_{24}B_2CoF_8N_8{\cdot}2H_2O$: C 47.1, H 3.7, N 14.7, B 2.8, Co 7.7%. Found: C 47.6, H 3.2, N 14.4, B 2.7, Co 8.1%. HRMS (+ESI, *m/z*): calcd. for $C_{30}H_{24}N_8BF_4Co^+$ (i.e., $[M^{2+} + BF_4^-]$) 642.1480, found 642.1480 (100%); $C_{30}H_{24}N_8Co^{2+}$ (i.e., $[M^{2+}]$) 277.5723, found 277.5713 (80%); $C_{30}H_{23}N_8Co^+$ (i.e., $[M^{2+} - H^+]$) 554.1373, found 554.1367 (5%).

Physical Characterization: Infrared spectroscopy was carried out on a Thermo Scientific Nicolet iS50 IR spectrometer using attenuated total reflection mode. UV–vis spectroscopy was conducted on an Agilent Cary 60 UV–vis spectrophotometer using quartz cuvettes with 10 mm path length. Photoluminescence spectroscopy was performed on an Edinburgh Instruments Spectrofluorometer FS5 equipped with Visible PMT-900 detector for solution samples. Zeta potential was recorded by using a Malvern Zetasizer Nano ZS spectrometer using a red laser (632.8 nm). ^{1}H Nuclear magnetic resonance spectroscopy (NMR) spectra were recorded on a Bruker 500 MHz AVIII HD Smart Probe Spectrometer under standard conditions (298 K) unless otherwise indicated. All ^{1}H chemical shifts were reported in ppm and have been internally calibrated to H_2O or the residual protons of the deuterated solvent. Elemental analyses (CHN analysis using a Perkin-Elmer 240 Elemental Analyzer and ICP-OES using a Thermo Scientific iCAP 7400 ICP-OES Analyzer) were conducted by the Microanalysis Service of the Yusuf Hamied Department of Chemistry, University of Cambridge. TEM images were collected using a Thermo Scientific (FEI) Talos F200X G2 TEM operating at 80 kV. TEM images were acquired using a Ceta 16M CMOS camera. Samples were prepared by applying 5 µL of the suspended sample in aqueous solution onto continuous carbon 300 mesh Cu grids that were negative glow discharged using a Quorum Technologies GloQube. The size distribution analysis was conducted by counting over 100 particles from five different images.

Photocatalytic Experiment: g-N-CDs (usually 0.5 mg) were dissolved in 2.925 mL of solvent mixture (usually DMSO: H_2O, 1:1, v:v) containing TEOA (0.1 M) and placed in a glass photoreactor vial (7.74 mL total volume) charged with a magnetic stir bar. Then, freshly prepared 1 mM solution of molecular catalyst (CotpyR) in deionized (DI) water (usually 75 µL for 75 nmol) was added to reach 3 mL of reaction solution with 4.74 mL of headspace. The photoreactor was capped with a rubber septum and purged with CO_2 containing 2% CH_4 as an internal gas chromatography standard for 15 min. The photoreactor was then kept stirring at 600 rpm at 25 °C under simulated solar light (Newport Oriel, 100 mW cm^{-2}) equipped with an air mass 1.5 global (AM 1.5G) filter and a water filter to cut-off infrared radiation. The produced H_2 and CO gas was monitored periodically by sampling the headspace (50 µL) by gas chromatography. Liquid products were not observed by ion chromatography.

Gas Quantification: The evolved H_2 and CO gas were monitored by a Shimadzu Tracera GC-2010 Plus gas chromatograph (GC) equipped with a barrier discharge ionization detector, Hayesep D pre-column, and a RT-Molsieve 5A main column in order to separate H_2, O_2, N_2, CH_4 and CO. In a typical experiment, 50 µL of headspace gas containing 2% CH_4 as an internal standard from the photoreactor was injected using an air-tight syringe (Hamilton, GASTIGHT). Apart from H_2 and CO gas measurement, 0.14 µmol of CH_4 was also observed after 24 h of light irradiation in DMSO:H_2O (3 mL, 1:1 v:v) containing g-N-CDs (0.5 mg) even in absence of both CO_2 and co-catalysts, supporting formation of small amounts of CH_4 from decomposition of g-N-CDs. However, the amount of CH_4 from the decomposition of g-N-CDs was negligible compared to the 2% CH_4 internal standard using for the GC measurement and did therefore not affect the quantification of CO. For CH_4 measurement, pure CO_2 gas without an internal standard was used to avoid inaccurate quantification by the much larger internal standard peak on the GC trace.

Electrochemical Analysis: Electrochemical experiments were conducted in a single-compartment cell using an Ivium CompactStat potentiostat. A three electrode configuration with a glassy carbon electrode as a working electrode, a Pt mesh as a counter electrode, and a Ag/AgCl, KCl (saturated) reference electrode was employed. Cyclic voltammetry (CV) scans of g-N-CDs (1 mg mL^{-1}), CotpyR (1 mM), and their mixture were recorded at 100 mV s^{-1} in a DMSO:H_2O (1:1 v:v) solution containing tetrabutylammonium tetrafluoroborate ($TBABF_4$, 0.1 M) as supporting electrolyte. The solution was purged with either N_2 or CO_2 for 15 min before the CV measurement and reference electrode was referenced against the ferrocene couple (Fc^+/Fc) for organic-water mixtures.

In-Situ UV–vis spectroscopy: In-situ UV–vis spectroscopy was carried out using an Agilent Cary 60 UV–vis spectrophotometer equipped with a homemade LED (405 nm) irradiation setup at 90° next to a sample holder, which was vertically placed against the detector. A quartz cuvettes capped with a rubber septum was charged with a DMSO:H_2O solution usually containing 0.1 M TEOA, g-N-CDs (0.1 mg), CotpyR (500 nmol) and $FeCl_3$ (500 nmol) and then purged with CO_2 for 15 min. The absorbance of the solution was periodically monitored under LED illumination.

Isotopic Labelling Experiment: g-N-CDs (0.5 mg) and $CotpyNH_2$ (75 nmol) dissolved in 3 mL of DMSO:H_2O or DMF:H_2O (1:1 v:v) solution containing 0.1 M TEOA was placed in a glass photoreactor vial (7.74 mL total volume) equipped with a magnetic stir bar. The photoreactor vial was capped with a rubber septum and degassed for 5 min. Next, $^{13}CO_2$ (1 bar) was gently introduced to the reaction vial. The photoreactor was irradiated (100 mW cm^{-2}) at 25 °C and stirred at 600 rpm for 24 h. The evolved gas in the headspace was transferred to an air-tight evacuated IR cell (10 cm path length with KBr windows) to detect the produced ^{13}CO with the background correction (IR cell under vacuum).

Statistical Analysis: All measured data were analyzed and plotted using Origin Pro (2021b, Origin Lab Corp.). Experiments were performed in triplicate and the values are presented as mean and standard deviation.

Supporting Information

Supporting Information is available from the Wiley Online Library or from the author.

Acknowledgements

The authors acknowledge support from the UKRI (ERC Advanced Grant, EP/X030563/1), the Swiss National Science Foundation (Early.Postdoc Fellowship: P2EZP2_191791), the European Commission for Horizon 2020 Marie Skłodowska-Curie Individual Fellowships (GAN891338 and 890745-SmArtC), and a Cambridge Trust scholarship (HRH The Prince of Wales Commonwealth Scholarship). Dr. Heather Greer is acknowledged for assistance with electron microscopy (EPSRC; EP/P030467/1), and Miss Ava Lage for helpful feedback and discussions.

Conflict of Interest

The authors declare no conflict of interest.

Data Availability Statement

Data supporting the findings of this study are available from the Cambridge data repository.[46]

Keywords

carbon dots, CO_2 reduction, material-molecule interfaces, molecular catalysts, photocatalysis

Received: January 31, 2024
Revised: February 7, 2024
Published online: March 22, 2024

[1] A. Gulzar, A. Gulzar, M. B. Ansari, F. He, S. Gai, P. Yang, *Chem. Eng. J. Adv.* **2020**, *3*, 100013.
[2] K. E. Dalle, J. Warnan, J. J. Leung, B. Reuillard, I. S. Karmel, E. Reisner, *Chem. Rev.* **2019**, *119*, 2752.
[3] M. A. Gross, A. Reynal, J. R. Durrant, E. Reisner, *J. Am. Chem. Soc.* **2014**, *136*, 356.

[4] B. C. M. Martindale, G. A. M. Hutton, C. A. Caputo, E. Reisner, *J. Am. Chem. Soc.* **2015**, *137*, 6018.
[5] F. Wen, C. Li, *Acc. Chem. Res.* **2013**, *46*, 2355.
[6] Z. Han, F. Qiu, R. Eisenberg, P. L. Holland, T. D. Krauss, *Science* **2012**, *338*, 1321.
[7] Z. Guo, S. Cheng, C. Cometto, E. Anxolabéhère-Mallart, S.-M. Ng, C.-C. Ko, G. Liu, L. Chen, M. Robert, T.-C. Lau, *J. Am. Chem. Soc.* **2016**, *138*, 9413.
[8] G. Neri, M. Forster, J. J. Walsh, C. M. Robertson, T. J. Whittles, P. Farràs, A. J. Cowan, *Chem. Commun.* **2016**, *52*, 14200.
[9] M. F. Kuehnel, K. L. Orchard, K. E. Dalle, E. Reisner, *J. Am. Chem. Soc.* **2017**, *139*, 7217.
[10] S. Choi, Y.-J. Kim, S. Kim, H. S. Lee, J. Y. Shin, C. H. Kim, H.-J. Son, S. O. Kang, *ACS Appl. Energy Mater.* **2022**, *5*, 10526.
[11] E. Lam, E. Reisner, *Angew. Chem., Int. Ed.* **2021**, *60*, 23306.
[12] C. Cometto, R. Kuriki, L. Chen, K. Maeda, T.-C. Lau, O. Ishitani, M. Robert, *J. Am. Chem. Soc.* **2018**, *140*, 7437.
[13] R. Kuriki, K. Sekizawa, O. Ishitani, K. Maeda, *Angew. Chem., Int. Ed.* **2015**, *54*, 2406.
[14] J. Liu, Y. Liu, N. Liu, Y. Han, X. Zhang, H. Huang, Y. Lifshitz, S.-T. Lee, J. Zhong, Z. Kang, *Science* **2015**, *347*, 970.
[15] T. S. Teets, D. G. Nocera, *Chem. Commun.* **2011**, *47*, 9268.
[16] B. Ma, G. Chen, C. Fave, L. Chen, R. Kuriki, K. Maeda, O. Ishitani, T.-C. Lau, J. Bonin, M. Robert, *J. Am. Chem. Soc.* **2020**, *142*, 6188.
[17] S. N. Baker, G. A. Baker, *Angew. Chem., Int. Ed.* **2010**, *49*, 6726.
[18] L. Đorđević, F. Arcudi, M. Cacioppo, M. Prato, *Nat. Nanotechnol.* **2022**, *17*, 112.
[19] M. Han, S. Zhu, S. Lu, Y. Song, T. Feng, S. Tao, J. Liu, B. Yang, *Nano Today* **2018**, *19*, 201.
[20] B. Domingo-Tafalla, E. Martínez-Ferrero, F. Franco, E. Palomares-Gil, *Molecules* **2022**, *27*, 1081.
[21] H. Yu, R. Shi, Y. Zhao, G. I. N. Waterhouse, L.-Z. Wu, C.-H. Tung, T. Zhang, *Adv. Mater.* **2016**, *28*, 9454.
[22] C. Ma, Z. Xie, W. C. Seo, S. T. Ud Din, J. Lee, Y. Kim, H. Jung, W. Yang, *Appl. Surf. Sci.* **2021**, *565*, 150564.
[23] J. Zhang, J. Xu, F. Tao, *ACS Appl. Energy Mater.* **2021**, *4*, 13120.
[24] S. Li, K. Ji, M. Zhang, C. He, J. Wang, Z. Li, *Nanoscale* **2020**, *12*, 9533.
[25] H. Zhong, R. Sa, H. Lv, S. Yang, D. Yuan, X. Wang, R. Wang, *Adv. Funct. Mater.* **2020**, *30*, 2002654.
[26] Y. Wang, X. Liu, X. Han, R. Godin, J. Chen, W. Zhou, C. Jiang, J. F. Thompson, K. B. Mustafa, S. A. Shevlin, J. R. Durrant, Z. Guo, J. Tang, *Nat. Commun.* **2020**, *11*, 2531.
[27] W.-J. Ong, L. K. Putri, Y.-C. Tan, L.-L. Tan, N. Li, Y. H. Ng, X. Wen, S.-P. Chai, *Nano Res.* **2017**, *10*, 1673.
[28] V. M. Badiani, C. Casadevall, M. Miller, S. J. Cobb, R. R. Manuel, I. A. C. Pereira, E. Reisner, *J. Am. Chem. Soc.* **2022**, *144*, 14207.
[29] B. C. M. Martindale, G. A. M. Hutton, C. A. Caputo, S. Prantl, R. Godin, J. R. Durrant, E. Reisner, *Angew. Chem., Int. Ed.* **2017**, *56*, 6459.
[30] J. Liu, N. Wang, Y. Yu, Y. Yan, H. Zhang, J. Li, J. Yu, *Sci. Adv.* **2017**, *3*, e1603171.
[31] J. J. Leung, J. Warnan, K. H. Ly, N. Heidary, D. H. Nam, M. F. Kuehnel, E. Reisner, *Nat. Catal.* **2019**, *2*, 354.
[32] E. C. Constable, K. Harris, C. E. Housecroft, M. Neuburger, J. A. Zampese, *Dalton Trans.* **2011**, *40*, 11441.
[33] D. S. Achilleos, W. Yang, H. Kasap, A. Savateev, Y. Markushyna, J. R. Durrant, E. Reisner, *Angew. Chem., Int. Ed.* **2020**, *59*, 18184.
[34] M. Abdellah, A. M. El-Zohry, L. J. Antila, C. D. Windle, E. Reisner, L. Hammarström, *J. Am. Chem. Soc.* **2017**, *139*, 1226.
[35] S. Roy, M. Miller, J. Warnan, J. J. Leung, C. D. Sahm, E. Reisner, *ACS Catal.* **2021**, *11*, 1868.
[36] D. Kim, M. Gu, Y. Choi, H. Kim, J. Ryu, B.-S. Kim, *ACS Appl. Energy Mater.* **2020**, *3*, 7103.
[37] Y. Wang, X.-W. Gao, J. Li, D. Chao, *Chem. Commun.* **2020**, *56*, 12170.
[38] N. Elgrishi, M. B. Chambers, V. Artero, M. Fontecave, *Phys. Chem. Chem. Phys.* **2014**, *16*, 13635.
[39] S. Roy, E. Reisner, *Angew. Chem., Int. Ed.* **2019**, *58*, 12180.
[40] B. Li, L. Sun, J. Bian, N. Sun, J. Sun, L. Chen, Z. Li, L. Jing, *Appl. Catal. B* **2020**, *270*, 118849.
[41] Q.-Q. Bi, J.-W. Wang, J.-X. Lv, J. Wang, W. Zhang, T.-B. Lu, *ACS Catal.* **2018**, *8*, 11815.
[42] V. Strauss, J. T. Margraf, C. Dolle, B. Butz, T. J. Nacken, J. Walter, W. Bauer, W. Peukert, E. Spiecker, T. Clark, D. M. Guldi, *J. Am. Chem. Soc.* **2014**, *136*, 17308.
[43] N. Elgrishi, M. B. Chambers, M. Fontecave, *Chem. Sci.* **2015**, *6*, 2522.
[44] T. Lawson, A. S. Gentleman, J. Pinnell, A. Eisenschmidt, D. Antón-García, M. H. Frosz, E. Reisner, T. G. Euser, *Angew. Chem., Int. Ed.* **2023**, *62*, e202214788.
[45] C. D. Sahm, G. M. Ucoski, S. Roy, E. Reisner, *ACS Catal.* **2021**, *11*, 11266.
[46] Research data supporting this work ca be found on the Apollo Repository, University of Cambridge, https://doi.org/10.17863/CAM.105945.